ChemComm

COMMUNICATION

View Article Online
View Journal | View Issue

Cite this: *Chem. Commun.*, 2023, **59**, 5265

Received 1st March 2023,
Accepted 18th March 2023

DOI: 10.1039/d3cc01037f

rsc.li/chemcomm

A photochromic metallacycle with highly anisotropic Dy–F magnetic units†

Nour El Beyrouti,[a] Felix Houard,[a] Marie Cordier,[a] Elzbieta Trzop,[b] Stéphane Rigaut,[a] Boris Le Guennic,[a] Kevin Bernot[a] and Lucie Norel*[a]

A dinuclear metallacycle assembled from a bispyridyl dithienylethene linker and a highly anisotropic dysprosium based Single Molecule Magnet (SMM) shows magnetic hysteresis at 1.8 K together with photoisomerization in single crystals (SC). The impact of photoswitching on the SMM behavior is evidenced and related to the specific organization of the magnetic units.

The large magnetic anisotropy exhibited by specific lanthanide complexes is the origin of SMM behaviour, characterized by long relaxation times of the magnetization and eventually magnetic hysteresis at temperatures ranging from liquid helium to liquid nitrogen.[1] Such a property, combined with the quantic nature of the complexes opens new possibilities in various fields such as spintronic.[2] In addition, the molecular nature of these architectures makes the introduction of other functions straightforward, therefore, extending the scope of possible applications.[3] For instance, the combination of SMM behaviour and light remote control can be targeted through simple association of an anisotropic magnetic building unit and a photoactive ligand,[3b,c] such as a photochromic dithienylethene derivative[4] that can undergo reversible transformation between two, so called, open and closed isomers.

Recently, we have used such an approach to obtain magnetic hysteresis photomodulation within chains of lanthanide single-molecule magnets having Dy(Tp^{py})F (Tp^{py} = tris(3-(2-pyridyl)pyrazolyl)hydroborate) magnetic units and bispyridyl terminated dithienylethene (DTE) photoswitches (compound **Dy-1D** in Fig. 1).[5]

In the present work, we investigate how the synthetic versatility of this unprecedented approach can be exploited to generate other topologies and draw structure–property relationships concerning this photomagnetic effect. More specifically, in comparison with **Dy-1D**,[5] we have used 1,2-bis(2-methyl,5-(3-pydidyl)-3-thienyl)perfluorocyclopentene,[6] **L** (Fig. 2), instead of the analogous 4-pyridyl terminated ligand. The result is a cyclic dinuclear coordination compound, able to isomerize in SC and with a photomagnetic response markedly different from **Dy-1D** despite a similar metal coordination sphere. This study thus underlines the importance of crystal packing and its modification under light irradiation as the main parameter triggering the changes in the magnetic hysteresis response.

The title compound and its yttrium analogue were obtained by combination of the DTE ligand in its closed state $\mathbf{L_c}$ and [M(Tp^{py})F(pyridine)$_2$]BArF (M = Y, Dy). These new precursors are easily synthesized by salt metathesis from the corresponding [M(Tp^{py})F(pyridine)$_2$]PF_6 complexes[7] (see ESI†). They undergo the same exchange reaction of the coordinated pyridines with ditopic ligands, as previously obtained for **Dy-1D**,[5] but the topology of the DTE linker induces here the formation of dinuclear rings rather than chains. The metallacycles obtained for both M = Dy (**1c**) and Y (**2c**), from slow evaporation of dichloromethane/hexane solutions, are isostructural (Table S3, ESI†). As a representative example, the X-ray structure of **1c** reveals an asymmetric unit composed of one dysprosium atom coordinated to the Tp^{py} ligand, one terminal fluoride atom and one pyridine group from the DTE ligand as well as a BArF anion. The ring structure is generated through an inversion center (space group $P\bar{1}$) located in the center of the ring and disposes the two Dy–F bonds exactly antiparallel, with a Dy–Dy distance of 12.279 Å (Fig. 1). The cavity resulting from the ring formation is filled with residual electronic

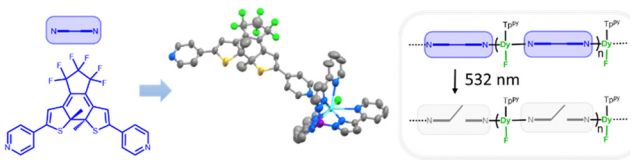

Fig. 1 previously investigated **Dy-1D** compound.

[a] *Univ Rennes, INSA Rennes, CNRS, ISCR (Institut des Sciences Chimiques de Rennes) – UMR 6226, F-35000 Rennes, France. E-mail: lucie.norel@univ-rennes1.fr*
[b] *Univ Rennes, CNRS, IPR (Institut de Physique de Rennes) – UMR 6251, F-35000 Rennes, France*

† Electronic supplementary information (ESI) available. CCDC 2221723, 2239099, 2239100, 2207245 and 2207246. For ESI and crystallographic data in CIF or other electronic format see DOI: https://doi.org/10.1039/d3cc01037f

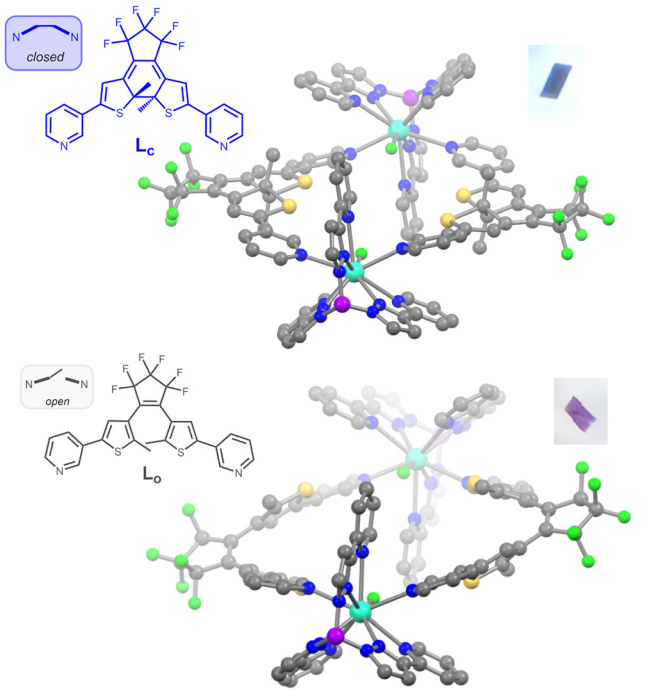

Fig. 2 Views of the dicationic dinuclear metallacycles in compounds **1c** (top, 150 K) and **1o** (bottom, 90 K) as determined from single-crystal X-ray diffraction data. Grey, blue, red, purple, green, yellow and light blue spheres represent C, N, O, B, F, S and Dy atoms respectively; H atoms are omitted for clarity. Insets show photographs of the crystals.

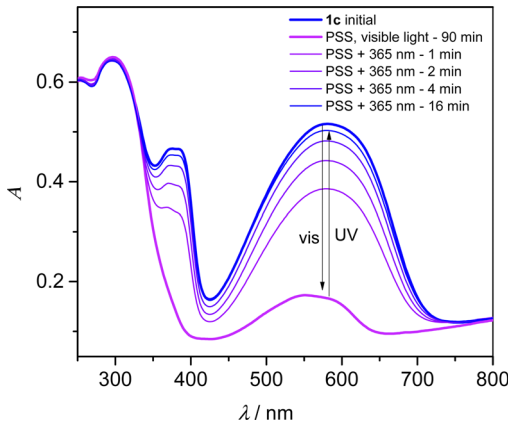

Fig. 3 Electronic absorption spectra (KBr pellet) of **1c** (blue line), the PSS after 90 min white light irradiation causing the opening reaction (purple line) and successively 1–16 min 365 nm irradiation causing the closing reaction.

density (likely from solvent molecules) that we could not satisfyingly model.

As a result of ring formation, the geometry around the dysprosium ion is a 9 coordinated spherical capped square antiprism as shown by the SHAPE analysis,[8] with a parameter of 0.863 for this geometry, consistent with the previous description of $[Dy(Tp^{py})F(pyridine)_2]PF_6$ (0.912)[7] and **Dy-1D** (0.731).[5] The main distortion to this ideal geometry comes from the very short Dy–F distance of 2.105(3) Å, which is expected to generate a strong axial magnetic anisotropy on each Dy center. The identification of bulk samples of **1c**/**2c** as having the formula $[(M(Tp^{py})F)_2(L_c)_2](BArF)_2$ is supported by elemental analysis, mass spectrometry, powder XRD data, as well as IR spectroscopy and, in the case of **2c**, NMR spectroscopy.

Since dithienylethene undergo solid-state photochromism, we have studied the isomerization reaction in KBr pellets. A pellet containing **1c** showed a deep blue color caused by a strong absorption band centered at 582 nm (Fig. 3). Together with the contribution at 374 nm, this band is the signature of the DTE linker in its closed state,[6] whereas the $DyTp^{py}F$ unit is expected to absorb light only in the UV region of the spectrum. Upon white light irradiation for 90 min, the pellet became pale violet and the bands of the closed DTE are replaced by a weaker contribution with λ_{max} = 552 nm in the photostationnary state (PSS). The initial blue color was restored upon irradiation at λ = 365 nm with a recovery of the initial spectrum of about 97% in intensity at 582 nm. Up to seven cycles of white light and UV exposure were successively performed without apparent fatigability due to degradation (Fig. S11, ESI†). The exact same behaviour was also observed for **2c** (Fig. S10 and S12, ESI†). However, the full opening of a DTE linker[5] under visible light irradiation is usually expected to lead to a colourless compound, and not the purple color obtained in the PSS.

To gain insights into this intriguing feature, TD-DFT calculations were performed on all possible isomers of the yttrium dinuclear structure (see ESI†). As expected, and after full geometry optimization (Fig. S30, ESI†), the calculated absorption spectrum for $[(Y(Tp^{py})F)_2(L_c)_2]^{2+}$ is consistent with the experimental behaviour, and a transition with π–π* character is calculated at λ_{max} = 609 nm (Table S14 and Fig. S31, ESI†). Similarly, the calculated spectrum for $[(Y(Tp^{py})F)_2(L_o)_2]^{2+}$ has no absorption in the visible range. We also constructed and optimized the geometry of a dinuclear complex having only one closed isomer, with formula $[(Y(Tp^{py})F)_2(L_o)(L_c)]^{2+}$ and observed a shift of the main π–π* transition to higher energy with λ_{max} = 602 nm (Table S14 and Fig. S32, ESI†), probably due to the distorsion of the conjugated path of the closed DTE upon the opening of the first ligand. Altholugh this calculated shift is smaller than observed, we can tentatively assign the purple color to residual highly colored closed DTE units from a partially isomerized structure, influenced also by crystal packing inducing further distortion of the closed DTE.

To further characterize the photoinduced open state, we first performed the isomerization reaction within SC. Upon 6h30 laser irradiation at λ = 660 nm (2.5 mW) of a batch of crystals of **1c**, purple crystals were obtained and remained of sufficient integrity to allow for structural determination. The space group remains $P\bar{1}$ after irradiation and the unit cell parameters show small variations upon light irradiation (Table S4, ESI†). The asymmetric unit is similar to the one of **1c** but the DTE ligand is now in its open state (Fig. 1), as clearly seen from the opening of the 6-membered ring and the lengthening of the reactive carbon atoms distance from 1.51 to 3.38 Å. Thus, complete isomerization to the open isomer is observed in SC and the compound is named **1o** (for "open"). Complementary evidence of full conversion comes from the ^1H and ^{19}F NMR analysis of a batch of **2c** crystals, crushed and exposed to white light for 92 h until its absorption spectrum matches the one

of the PSS. At this stage, the compound was dissolved in CD_3OD, causing decoordination and formation of $[Y(Tp^{py})F(CD_3OD)_2]^+$, $BArF^-$ and free DTE ligand (Fig. S16–S18, ESI†). The spectral signature of the later clearly indicates the presence of the open form with less than 1% of the closed form remaining after irradiation. Thus the PSS corresponds to an almost fully isomerized ring structure with formula $[(M(Tp^{py})F)_2(L_o)_2](BArF)_2$ for **1o** (M = Dy) and **2o** (M = Y). Finally, only the opening reaction could be followed on SC but not the subsequent closing reaction since UV irradiation reduced the sample crystallinity.

Since our working hypothesis for SMM photo-modulation is that the crystal packing modification upon isomerisation can influence the magnetic properties, it is important to compare in details the structures of **1c** and **1o**. Concerning the dysprosium coordination sphere, it stays almost perfectly identical upon isomerization, as shown by the SHAPE parameter of 0.754 for **1o** for the spherical capped square antiprism geometry and the overlay of the two coordination spheres (Fig. S4, ESI†). The Dy–F distance in **1o** is the same as in **1c** within experimental error (2.107(4) Å). We thus expect that crystal field splitting will be the same for **1c** and **1o** and will be comparable to the one observed for $[Dy(Tp^{py})F(pyridine)_2]PF_6$[7] or **Dy-1D**,[5] with a total splitting of 800 cm^{-1} and a first excited state at around 300 cm^{-1}. The Dy-Dy distance within the ring is larger in **1o** with 13.079 Å (+0.80 Å) and the antiparallel disposition of the Dy–F dipoles persists (Fig. S5, ESI†). Actually, the closest Dy–Dy distance is the result of π stacking existing between adjacent pyrazolylpyridine arms and varies only slightly from 8.624 Å in **1c** to 8.630 Å in **1o** (Fig. S6, ESI†). The next closest Dy–Dy distance of 10.710 Å in **1c** becomes shorter in **1o** with 10.376 Å (−0.334 Å). These distances correspond to perfect antiparallel disposition of the Dy–F dipoles and thus potential antiferromagnetic dipolar couplings contrary to **Dy-1D** where ferromagnetic interactions were calculated.

The rings in **1o** are heterochiral with two DTE with opposite helicity (M and P), since the homochiral arrangement is not compatible with the cyclic arrangement. Since each helicity of the open DTE is stereoselectively obtained from a given disposition of the methyl groups in the closed state, with for instance the M helix resulting from the opening of the (*S*,*S*) configuration of the chiral carbon centers, it means that starting closed compound **1c** also shows heterochiral (*R*,*R*), (*S*,*S*) ring structures, probably induced by the crystalisation process from a mixture of several stereoisomers in dynamic equilibrium. Indeed, the inversion center in **1c** imposes the heterochiral disposition of the DTE even if the methyl groups of the DTE show substantial crystallographic disorder modelled with 3 possible dispositions roughly corresponding to the two enantiomers of the DTE in a 47.9 to 52.1% ratio.

Compounds **1c** and **1o** were then characterized in the solid state by static (dc) and dynamic (ac) magnetization measurements (Fig. S22–S29 and Table S5–S13, ESI†). The room temperature $\chi_M T$ values for both **1c** and **1o** (28.30 and 28.50 emu K mol^{-1}, respectively) are close to the predicted value of 28.34 emu K mol^{-1} for a dinuclear system with isolated Dy^{3+} ions ($^6H_{15/2}$, $S = 5/2$, $L = 5$, and $g = 4/3$) and are in excellent agreement with previously investigated compounds of this family. These $\chi_M T$ values start to decrease steadily below 200 K, before dropping dramatically below 3.5 K mainly because of saturation effect.

$$\tau^{-1} = BT^n + \tau_0^{-1} \exp(-U_{eff}/k_B T) + \tau_{tunnel}^{-1} \quad (1)$$

The ac magnetic susceptibility measurements for both compounds exhibited peaks in the out-of-phase susceptibility (χ''_M) *vs.* frequency curves at temperatures up to 46 K, in the absence of an applied dc field. The low temperature peaks exhibit little temperature dependence and as a result the Arrhenius plot (Fig. 4) of the relaxation times *versus* inverse temperature shows a plateau at the lowest temperature. This behaviour is consistent with quantum tunnelling as the primary magnetic relaxation pathway in the 2–6 K range for both compounds but with a slightly faster relaxation in the case of **1o** compared with **1c** (0.495 s and 0.140 s at 2 K respectively). At higher temperature, a shift of the out-of-phase peaks with temperature is observed, consistent with Raman and Orbach relaxation processes taking over upon rising the temperature. It is striking that the relaxation time for **1o** and **1c** tend to merge when the temperature is above 20 K meaning that the Orbach regime is common to both compounds. Actually, upon application of a dc field of 1600 Oe, which was determined to be optimal for slowing down the magnetic relaxation for both compounds, the data collected in the 0.7–1500 Hz window are nearly identical (within error) for **1c** and **1o**, underlying that the main difference in their behaviour is the quantum tunnelling rate. Therefore, we fitted the temperature dependence of the relaxation time using the eqn (1) which includes Raman, Orbach and quantum tunnelling contributions.

In line with our observation, unique parameters where used to fit the Orbach regime for both compounds in both applied fields. The quantum tunnelling parameters were fixed to zero for 1600 Oe applied field and Raman parameters were optimized in all cases. The result of this fitting procedure is shown in Table 1 (0 Oe) and Table S13 (ESI†) (1600 Oe). The relaxation barrier of 193 cm^{-1} agrees well with the ones previously determined for compounds with similar coordination spheres (like **Dy-1D**) and are probably underestimated by the fitting procedure since *ab initio* calculations

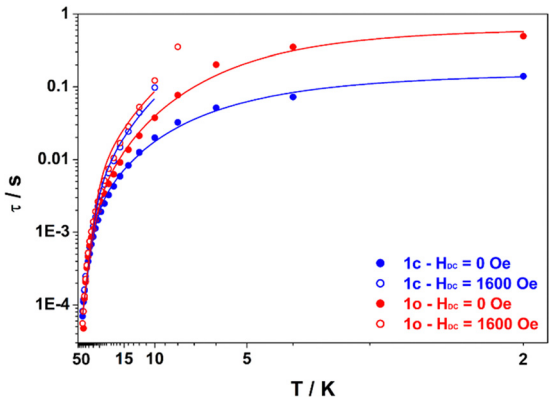

Fig. 4 Plot of the relaxation time τ (log scale) *versus* *T* (inverse scale) for **1c** (blue) and **1o** (red) measured under H_{DC} = 0 Oe (full dots) and H_{DC} = 1600 Oe (open dots). Lines are best fits according to eqn (1) assuming fixed values of U_{eff} = 193 cm^{-1} and $\tau_0 = 1.86 \times 10^{-7}$ s for both compounds with the parameters from Table 1 (0 Oe) and Table S13 (ESI†) (1600 Oe).

Table 1 Parameters extracted from the fitting of the Arrhenius plots of **1c** and **1o** under 0 Oe external dc field according to eqn (1). See ESI for details of the fitting procedure and parameters for measurement under 1600 Oe external dc field

	1c	**1o**
U_{eff} (cm^{-1})	193 (±17)	
τ_0 (10^{-7} s)	1.86 (±0.35)	
τ_{QT} (s)	0.16 (±0.03)	0.66 (±0.21)
B (s^{-1} K^{-n})	0.22 (±0.08)	0.030 (±0.016)
n	2.36 (±0.12)	2.90 (±0.19)

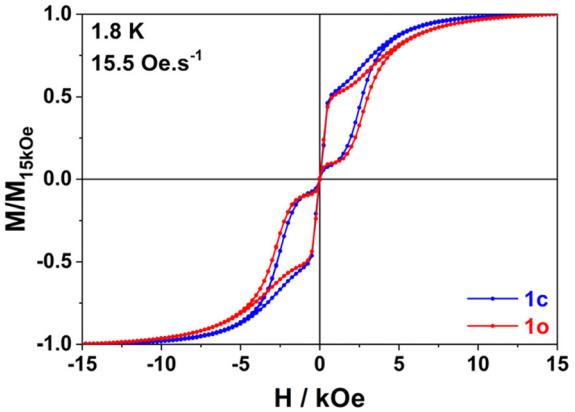

Fig. 5 Variable field magnetization data for **1c** (blue) and **1o** (red) collected at 1.8 K using a field sweep rate of 15.5 Oe min^{-1}. Data are normalized on the basis of the magnetization value measured at 15 kOe.

predict 282 cm^{-1} for a virtually identical coordination sphere in $[Dy(Tp^{py})F(pyridine)_2]PF_6$.[7] This barrier remains constant upon isomerization in agreement with the coordination sphere upholding (see supra). Finally, the major effect of isomerization is the slowing down of quantum tunneling roughly by a factor of 4 and overall, these parameters make the relaxation behaviour of both **1c** and **1o** slower than that of **Dy-1D** for which the limiting tunnelling time was at best 0.0337 s. Variable-field magnetization data collected for **1c** and **1o** at 1.8 K revealed the presence of butterfly magnetic hysteresis similar to that observed for previous complexes of this family (Fig. 5).[5] As expected from the limited changes in the different parameters describing the relaxation processes, the hysteresis curves of **1c** and **1o** show pretty much the same characteristics and unlike the behavior of **Dy-1D**, the DTE opening does not cause a shrinking of the hysteresis loop.

We link hysteresis persistence under light-switching to several parameters. First, the unchanged coordination sphere of the dysprosium ion lead to the same energy barrier for the Orbach process. Second, the Raman parameters are not dramatically changed. However, these two observations also hold for **Dy-1D** and this compound clearly shows larger changes in its hysteresis. So, the main difference between these two cases comes from the reduced influence of the opening reaction on quantum tunnelling (÷22 in **Dy-1D**, ×4 in **1**) that can be tentatively linked with the changes in dipolar couplings. Indeed, for **1** the shorter Dy–Dy distance is almost unchanged during the isomerization process (+0.006 Å) contrary to what is seen on **Dy-1D** (−0.107 Å). This means that the main contribution to the change in dipolar coupling is here cancelled.

To conclude, our versatile synthetic approach allows the synthesis of chains as well as unprecedented ring structures having two anisotropic dysprosium centers linked by DTE units. The linker opening reaction proceed in SC with full conversion and crystal structure was determined on both photo-isomers. However, unlike its chain analogue, this is not accompanied by important changes in the slow relaxation dynamics, as a result of the specific packing and arrangement of dysprosium atoms in this structure that ensure a very robust magnetic behaviour, with only marginal modification of dipolar interactions. We are currently investigating how other photochromic switches can lead to coordination compounds combining crystal tolerance to photoisomerization with significant changes in their magnetic behaviour.

Conflicts of interest

There are no conflicts to declare.

Notes and references

1 (*a*) C. Benelli and D. Gatteschi, *Introduction to Molecular Magnetism, From transition metals to lanthanides*, Wiley-VCH, Weinheim, Germany, 2015; (*b*) K. L. M. Harriman, D. Errulat and M. Murugesu, *Trends Chem.*, 2019, **1**, 425–439; (*c*) N. Ishikawa, M. Sugita, T. Ishikawa, S. Koshihara and Y. Kaizu, *J. Am. Chem. Soc.*, 2003, **125**, 8694–8695; (*d*) F.-S. Guo, B. M. Day, Y.-C. Chen, M.-L. Tong, A. Mansikkamäki and R. A. Layfield, *Science*, 2018, **362**(6421), 1400; (*e*) C. A. P. Goodwin, *Dalton Trans.*, 2020, **49**, 14320–14337.
2 (*a*) S. Sanvito, Molecular spintronics, *Chem. Soc. Rev.*, 2011, **40**, 3336–3355; (*b*) E. Coronado, *Nat. Rev. Mater.*, 2020, **5**, 87–104.
3 (*a*) O. Cador, B. Le Guennic and F. Pointillart, *Inorg. Chem. Front.*, 2019, **6**, 3398–33417; (*b*) Z. Zhu, X.-L. Li, S. Liu and J. Tang, *Inorg. Chem. Front.*, 2020, **7**, 3315–3326; (*c*) M. Feng, Z.-Y. Ruan, Y.-C. Chen and M.-L. Tong, *Chem. Commun.*, 2020, **56**, 13702–13718.
4 (*a*) M. Irie, T. Fulcaminato, K. Matsuda and S. Kobatake, *Chem. Rev.*, 2014, **114**(24), 12174–12277; (*b*) D. Pinkowicz, M. Ren, L. M. Zheng, S. Sato, M. Hasegawa, M. Morimoto, M. Irie, B. K. Breedlove, G. Cosquer, K. Katoh and M. Yamashita, *Chem. – Eur. J.*, 2014, **20**(39 12502–12513; (*c*) K. Rogacz, M. Brzozowska, S. Baś, K. Kurpiewska and D. Pinkowicz, *Inorg. Chem.*, 2022, **61**(41), 16295–16306.
5 M. Hojorat, H. Al Sabea, L. Norel, K. Bernot, T. Roisnel, F. Gendron, B. Le Guennic, E. Trzop, E. Collet, J. R. Long and S. Rigaut, *J. Am. Chem. Soc.*, 2019, **142**, 931–936.
6 S.-C. Wei, M. Pan, Y.-Z. Fan, H. Liu, J. Zhang and C.-Y. Su, *Chem. – Eur. J.*, 2015, **21**, 7418–7427.
7 L. Norel, L. E. Darago, B. Le Guennic, K. Chakarawet, M. I. Gonzalez, J. H. Olshansky, S. Rigaut and J. R. Long, *Angew. Chem., Int. Ed.*, 2018, **57**, 1933–1938.
8 A. Ruiz-Martínez, D. Casanova and S. Alvarez, *Chem. – Eur. J.*, 2008, **14**, 1291–1303.

